

# Journal of Materials Chemistry A

Accepted Manuscript



This is an *Accepted Manuscript*, which has been through the Royal Society of Chemistry peer review process and has been accepted for publication.

*Accepted Manuscripts* are published online shortly after acceptance, before technical editing, formatting and proof reading. Using this free service, authors can make their results available to the community, in citable form, before we publish the edited article. We will replace this *Accepted Manuscript* with the edited and formatted *Advance Article* as soon as it is available.

You can find more information about *Accepted Manuscripts* in the [Information for Authors](#).

Please note that technical editing may introduce minor changes to the text and/or graphics, which may alter content. The journal's standard [Terms & Conditions](#) and the [Ethical guidelines](#) still apply. In no event shall the Royal Society of Chemistry be held responsible for any errors or omissions in this *Accepted Manuscript* or any consequences arising from the use of any information it contains.

# Enhanced Thermoelectric Properties of PEDOT:PSS Nanofilms by Chemical Dedoping Process

Hongkwan Park<sup>a</sup>, Seung Hwan Lee<sup>a</sup>, Felix Sunjoo Kim<sup>b</sup>, Hyang Hee Choi<sup>a</sup>, In Woo Cheong<sup>c</sup>,  
and Jung Hyun Kim<sup>a,\*</sup>

<sup>a</sup>Department of Chemical and Biomolecular Engineering, Yonsei University, 50 Yonsei-ro,  
Seodaemun-gu, Seoul 120–749, Republic of Korea

<sup>b</sup>Department of Chemical Engineering and Materials Science, Chung-Ang University, 84  
Heukseok-ro, Dongjak-gu, Seoul 156–756, Republic of Korea

<sup>c</sup>Department of Applied Chemistry, Kyungpook National University, 80 Daehak-ro, Buk-gu,  
Daegu 702–701, Republic of Korea

Submitted to *Journal of Materials Chemistry A*

## \* Corresponding Authors

Jung Hyun Kim, Ph.D.

Department of Chemical and Biomolecular Engineering, Yonsei University, 50 Yonsei-ro,  
Seodaemun-gu, Seoul 120–749, Republic of Korea

Tel: +82-2-2123-7633; Fax: +82-2-312-0305; Email: jayhkim@yonsei.ac.kr

## Abstract

We report that a simple chemical dedoping treatment on poly(3,4-ethylenedioxythiophene):poly(styrenesulfonate) (PEDOT:PSS) nanofilms enhances the thermoelectric properties of the polymer nanofilms. The dedoping process was done by over-coating a mixture of dimethyl sulfoxide (DMSO) and hydrazine (HZ), a strong chemical reducing agent, onto the PEDOT:PSS nanofilms. This additional step led to the removal of excess PSS chains and the formation of neutral states of PEDOT chains, resulting in an improvement in the Seebeck coefficient, from 30  $\mu\text{V/K}$  to 142  $\mu\text{V/K}$ , and a decrease in the electrical conductivity from 726 S/cm to 2 S/cm. By controlling the concentration of HZ, we obtained an optimized power factor of 112  $\mu\text{W/mK}^2$  at 0.0175 wt% of HZ in DMSO at room temperature. The corresponding electrical conductivity and Seebeck coefficient at the optimized conditions were 578 S/cm and 67  $\mu\text{V/K}$ , respectively. We expect that this simple dedoping process can be applied to general thermoelectric nanofilms based on chemically doped polymers in order to enhance the power factor.

**Keywords:** thermoelectric, PEDOT:PSS, dedoping, over-coating method, nanofilms

## 1. Introduction

Efficient thermoelectric materials and devices that turn waste heat into clean electricity have become of great interest in energy research, ever since the possibility of high thermoelectric figure of merit ( $ZT$ ) was observed through a series of molecular and nanostructural engineering.<sup>1, 2</sup> The advancement of thermoelectric materials and processing has made the thermoelectric technology one of the promising next-generation energy sources, being comparable to other green-energy systems. The thermoelectric performance of materials is described by a  $ZT$  given by:

$$ZT = \sigma S^2 T / \kappa \quad (1)$$

where  $S$  stands for the Seebeck coefficient (also called the thermopower),  $\sigma$  and  $\kappa$  are the electrical and thermal conductivities, respectively, and  $T$  is the absolute temperature. Here, a product of an electrical conductivity and a square of the Seebeck coefficient is called a power factor ( $\sigma S^2$ ). To achieve a high  $ZT$  value, materials are required to have a high power factor and a low thermal conductivity. However, the conflicting combination among the electrical conductivity, the Seebeck coefficient, and the thermal conductivity imposes limitations on the optimization of  $ZT$ .<sup>3</sup> Traditional inorganic thermoelectric materials such as bismuth telluride ( $\text{Bi}_2\text{Te}_3$ ) have been widely studied for the applications at room temperature.<sup>1</sup> Despite the high power factor, these inorganic materials still face the challenges to decrease the thermal conductivity in order to enhance their thermoelectric energy conversion efficiency. Moreover,

inorganic thermoelectric materials have several disadvantages such as difficulty in processing, high cost in production, and environmental concerns due to their toxicity.

Recently, efforts have been focused on improving the thermoelectric properties of organic materials. Organic thermoelectric materials, conducting polymers in particular, have various advantages over inorganic materials. Electrical conductivity of organic materials can be widely tuned by chemical doping.<sup>4,5</sup> Low thermal conductivity of organic materials in general is crucial to achieve superior thermoelectric properties in devices.<sup>6,7</sup> The solubility of conducting polymers not only enables easy processing from solutions, but also allows blending or compositing of the materials with other organic/inorganic materials.<sup>8</sup> Due to such intrinsic advantages, significant breakthroughs in the thermoelectric properties of the conducting polymers are expected. Polypyrrole (PPy),<sup>9</sup> polyaniline (PANI),<sup>10,11</sup> polycarbazole,<sup>12</sup> and polythiophene<sup>13-15</sup> and its derivatives including poly(3,4-ethylenedioxythiophene) (PEDOT)<sup>16</sup> are among the promising conducting polymers.

PEDOT complexed with poly(4-styrenesulfonic acid) (PSS),<sup>6,17-20</sup> also called as PEDOT:PSS, has been studied as the most promising conducting polymers for thermoelectric applications because of its high electrical conductivity and environmental stability. The conductivity of PEDOT:PSS can be increased by several orders of magnitude by adding dielectric solvents such as dimethyl sulfoxide (DMSO) and ethylene glycol.<sup>21</sup> It has been reported that the addition of dielectric solvents results in aligning of the PEDOT chain and the

enhanced charge-carrier transport.<sup>22-24</sup> However, although recent progress in PEDOT:PSS nanofilms has showed remarkably enhanced power factors by chemically or electrochemically controlling their oxidation level<sup>19, 20</sup> and changing their physical structures with addition of dopants and solvents,<sup>26, 27, 28</sup> the power factor of PEDOT:PSS nanofilms is still suffer from a much lower Seebeck coefficient (below 20  $\mu\text{V/K}$ )<sup>6, 27</sup>, than inorganic and composite thermoelectric materials<sup>25, 29</sup>, resulting in a low  $ZT$  value at room temperature. Recently, it was shown that the thermoelectric properties of the PEDOT:PSS films could be enhanced by removing unionized portion of the PSS molecules, which reduces charge-carrier mobility, by immersing the film in a dielectric solvent, achieving a record value of  $ZT = 0.42$ .<sup>30</sup>

Herein, we report an optimization of a thermoelectric power factor ( $\sigma S^2$ ) of the PEDOT:PSS nanofilms obtained from *chemical* dedoping processes. Through chemical dedoping process with over-coating of a ratio-controlled mixture of DMSO and a dedoping agent (hydrazine; HZ), we have been able to change the doping level of PEDOT:PSS films and, at the same time, remove the unionized PSS molecules to control the electric conductivity and the Seebeck coefficient. By doing so, we have demonstrated a high power factor of 112  $\mu\text{W/mK}^2$  from the nanofilms of chemically-dedoped, in-house-synthesized PEDOT:PSS which is  $\sim 14$  times larger than that of the pristine PEDOT:PSS nanofilms in this study ( $\sim 8 \mu\text{W/mK}^2$ ). With a low intrinsic thermal conductivity of PEDOT:PSS nanofilms ( $\sim 0.31\text{--}0.37 \text{ W/mK}$ ),  $ZT$  has reached  $\sim 0.1$  at room temperature. The high  $ZT$  of the dedoped

PEDOT:PSS nanofilms provides promise for low-cost and large-area thermoelectric power generators. It is worth noting that, unlike the recent report<sup>30</sup> published while our manuscript was in preparation, we have demonstrated controlled dedoping of an organic thermoelectric system by adjusting one of the most common processing variables, i.e. concentration of the post-treatment solution. Our chemical dedoping approach has enabled a systematic study, which is complementary to the recent report,<sup>30</sup> as described below.

## 2. Experimental Section

**Materials:** Poly(4-styrenesulfonic acid) (PSS; 18 wt% in water), sodium persulfate ( $\text{Na}_2\text{S}_2\text{O}_8$ ;  $\geq 98\%$ ), 3,4-ethylenedioxythiophene (EDOT; 99%), iron (III) sulfate hydrate ( $\text{Fe}_2(\text{SO}_4)_3$ ; 97%) and hydrazine (HZ; 35 wt% solution in water) were purchased from Sigma-Aldrich (St Louis, MO, USA). Dimethyl sulfoxide (DMSO; 99%) was purchased from Samchun Pure Chemicals Co., LTD (Pyungtaek, Korea). Distilled de-ionized water was used throughout the experiments.

**Preparation of dedoped PEDOT:PSS Nanofilms:** PEDOT:PSS solutions with various compositions were prepared by using the Baytron synthesis procedure.<sup>31</sup> The ratio of PEDOT:PSS was controlled to be 1:0.8, 1:2.5, 1:6, and 1:7.5. DMSO was added to the PEDOT:PSS solutions to have 5% of DMSO and stirred at 50 °C for 3 hours before spin coating. PEDOT:PSS nanofilms were prepared by spin-coating the solution onto  $2.5 \times 2.5 \text{ cm}^2$

glass substrates, which were pre-cleaned sequentially with acetone, isopropyl alcohol, methyl alcohol, and DDI water. A PEDOT:PSS solution was dropped onto the glass substrate which was loaded on a spin coater (ACE-200, Dong Ah Tech) and then spun at 1000 rpm for 30 s. The PEDOT:PSS nanofilms were subsequently annealed on a hot plate at 150 °C for 10 min in air. For dedoping of PEDOT:PSS nanofilms, the HZ treatment was performed by spin-coating a HZ solution in DMSO or in water onto the nanofilm at 1000 rpm for 10 s. The dedoped PEDOT:PSS nanofilms were dried again for about 10 min at 150 °C to remove the residual solvent from the nanofilms and then cooled down to room temperature.

**Characterization:** The change of the conformation of PEDOT and PSS in the nanofilms was investigated by using Raman spectra (HORIBA JOBIN YVON; LabRam ARAMIS; Tokyo, Japan) with 532 nm (green) Nd:Yag laser excitation. The samples were examined under ambient conditions without any prior treatment. The surface images of the nanofilms were obtained by using an atomic force microscope (AFM, Park Systems XE-100) in non-contact mode. The elements and compounds in the PEDOT:PSS nanofilms were characterized by using X-ray photoelectron spectroscopy (XPS; Thermo K-Alpha XPS, Thermo Fisher Scientific, West Palm Beach, FL). To compensate for the effects of surface charges, all binding energies were referenced to the C 1s neutral carbon peak at 284.6 eV. The ultraviolet-visible-near-infrared (UV-Vis-NIR) absorption spectroscopy was performed at room temperature by using a PerkinElmer Lambda 750 spectrophotometer with the wavelength



ranging from 300 to 1200 nm. The electrical conductivity of the nanofilms was measured via the van der Pauw method with a four-point contact configuration by using a combination of a Keithley 2400 source-measure unit, a 2182 nanovoltmeter, and a 7001 switch system. The electrical contacts were made by applying gold electrodes (2 mm in width and 2 mm in length) for Ohmic contacts on size of  $1 \times 1 \text{ cm}^2$  the four-point of each PEDOT:PSS nanofilm on a glass substrate. The Seebeck coefficient was measured from the samples with the gold electrodes by using a home-built setup. This setup consisted of two Peltier devices to maintain a controlled temperature gradient. The Peltier devices were controlled by using a Keithley 2400 source-measure unit and a Keithley 2200-30-5 power supply. Two thermocouples were used to measure the temperature gradient across the PEDOT:PSS nanofilms. A thickness of the PEDOT:PSS nanofilm was measured by using the Alpha-Step 500 surface profiler (AS500; KLA-Tencor Co., USA). The thermal conductivity ( $\kappa$ ) was calculated from the measured thermal diffusivity ( $D$ ), specific heat ( $C_p$ ), and density ( $d$ ), according to the relationship  $\kappa = DC_p d$ . For thermal conductivity of the PEDOT:PSS, “through-plane” thermal diffusivity was measured with a 12.5 mm diameter disk (pellet using hot press pelletizer) by the Laser Flash Apparatus (LFA 457; Netzsch, Selb, Germany) methods based on xenon flash lamp source. The specific heat was determined by using a power-compensation differential scanning calorimeter (DSC; Q20, TA Instruments, New Castle, DE) in vacuum. All measurements were performed at room temperature.

### 3. Results and Discussion

**Figure 1** shows a schematic of the experimental procedure adopted for the preparation of PEDOT:PSS nanofilms using spin coating and dedoping (over-coating) processes. PEDOT:PSS nanofilms were deposited onto glass substrates by spin-coating an aqueous solution of the synthesized PEDOT:PSS with various PEDOT to PSS ratios of 1:0.8, 1:2.5, 1:6, and 1:7.5. The nanofilms were then annealed on a hot plate at 150 °C for 10 min to vaporize the residual solvent and DMSO, which was added as a conductivity enhancer in the stock solutions, and to change the polymer conformation from coiled to linear or expanded-coil structures. Finally, the deposited PEDOT:PSS nanofilms were post-treated with a mixture of DMSO/HZ by an over-coating method to control the chemical doping levels and induce morphological changes. Over-coating was simply done by spin-coating the dedoping agents (*i.e.* hydrazine mixed with DMSO with a controlled ratio in this study) onto the pre-deposited PEDOT:PSS nanofilms on a glass substrate. The over-coating method enables simple, fast, and controlled dedoping of the nanofilms.

To find an optimal composition of PEDOT:PSS nanofilms for thermoelectric applications, we have measured the electrical conductivity, the Seebeck coefficient, and the power factor of the nanofilms without dedoping process as a function of the PEDOT:PSS ratio (**Figure 2**). The conductivity was increased from 726 S/cm to 812 S/cm by controlling the PEDOT:PSS

ratio from 1:0.8 to 1:2.5, and then decreased to 6.5 S/cm with further increasing the PSS composition to 1:7.5 of the PEDOT:PSS ratio. The Seebeck coefficient was slightly decreased from 30.1  $\mu\text{V/K}$  to 21.3  $\mu\text{V/K}$  by varying PEDOT:PSS from 1:0.8 to 1:7.5. As a result, the highest power factor is 65  $\mu\text{W/mK}^2$  when the ratio of PEDOT:PSS was 1:0.8. The electrical conductivity and Seebeck coefficient decreased because of the presence of excessive PSS having a tendency to intertwine with PEDOT chain and limit charge-carrier transport in the nanofilms. Therefore, in the subsequent experiments of over-coating and dedoping, we used the PEDOT:PSS solution with the ratio of 1:0.8.

As shown in **Figure 3**, Raman spectra under excitation was 532 nm Nd:YAG laser confirmed a conformational change of PEDOT from coiled to linear or to expanded-coil structures occurred in the PEDOT:PSS nanofilms with DMSO addition and/or post-processing (i.e. over-coating of DMSO/HZ onto the nanofilms). The shoulder bands between 1400 and 1500  $\text{cm}^{-1}$  became weaker relative to the pristine PEDOT:PSS nanofilm after addition of the polar solvent (DMSO). Furthermore, the band of the dedoped PEDOT:PSS nanofilms after DMSO/HZ treatment was red-shifted and became narrower, suggesting that chemical dedoping (i.e. changing the doping states of PEDOT chains from (bi)polarons to neutral states) occurred while the resonant structure of PEDOT chain maintained the quinoid structure (**Figure 3c**). The bands at 991  $\text{cm}^{-1}$  corresponding to the deformations of oxyethylene ring, at 1121  $\text{cm}^{-1}$  for PSS component, and at 1261  $\text{cm}^{-1}$  corresponding to  $\text{C}_\alpha\text{-C}_\alpha$

inter-ring stretching vibrations were found in the pristine and DMSO-added PEDOT:PSS nanofilms, but were weaker or absent in the dedoped nanofilms treated by a mixture of DMSO/HZ. Especially, the reduction of the band at  $1121\text{ cm}^{-1}$  indicates that the PSS molecules are further removed during the over-coating process. The strong band of the dedoped nanofilms shifted from  $1445$  to  $1431\text{ cm}^{-1}$  and became narrower than the pristine and DMSO-added PEDOT:PSS nanofilms, indicating the decrease in the doping level from bipolaron to polaron or neutral by DMSO/HZ treatment. The peaks at  $1365\text{ cm}^{-1}$ ,  $1431\text{ cm}^{-1}$ ,  $1516\text{ cm}^{-1}$  are assigned to the  $C_{\beta}-C_{\beta}$  stretching deformation, the symmetric C=C in-plane stretch vibration, and the asymmetric C=C in-plane stretch vibration, respectively.<sup>32</sup> Moreover, the peak at  $1546\text{ cm}^{-1}$  was absent, and new peaks at  $1516$  and  $1555\text{ cm}^{-1}$  appeared in the dedoped PEDOT:PSS films. These results suggest that DMSO induces significant morphological change such as phase separation between PEDOT and PSS chains as well as elongation and conformational changes of the PEDOT chain, leading to enhancement of interchain interactions, carrier mobility, and electrical conductivity.<sup>32-36</sup> Furthermore, these results also suggest that HZ results in the dedoping of PEDOT chains into the chemically neutral states.

The AFM images of PEDOT:PSS nanofilms prepared by adding DMSO into the solution or by over-coating of DMSO/HZ onto the nanofilm were recorded to investigate possible changes in surface morphology (**Figures 4 and S1**). The topography images of a  $2\times 2\text{ }\mu\text{m}^2$

area of the pristine PEDOT:PSS nanofilm and the nanofilm with 5% DMSO treatment showed an increase in the surface root-mean-square roughness ( $R_q$ ) from 2.0 to 2.7 nm (**Figure 4a,b**). A similar effect on the morphology was found with over-coating of DMSO/HZ mixtures as shown in **Figure 4c**. The dedoped PEDOT:PSS films by a mixture of DMSO and HZ showed that bright PEDOT-rich regions evolved further compared to the DMSO-treated nanofilms.  $R_q$  became even larger from 2.7 to 3.1 nm after dedoping. These results indicate that the DMSO-added PEDOT:PSS nanofilms have larger conducting areas and thus improved conductivity as a result of the enlargement of the conducting PEDOT-rich core and the reduction of charge-transport barriers. Large portion of remained PSS-rich regions was further removed after over-coating with a mixture of DMSO and HZ.

To confirm the effects of the treatment on PEDOT:PSS nanofilms, the surface chemical compositions of the nanofilms were analyzed by X-ray photoelectron spectroscopy (XPS). **Figure 5** shows the XPS spectra of the PEDOT:PSS nanofilms before and after the treatment with DMSO and the mixture of DMSO/HZ. Two characteristic sulfur (S) 2p peaks were detectable in the PEDOT:PSS nanofilms, because the S atoms of thiophene in PEDOT and of sulfonate in PSS have different binding energies.<sup>24, 37, 38</sup> the lower energy peaks (164.6 and 163.4 eV) correspond to the S atoms in PEDOT and the higher energy peaks (169 and 167.8 eV) correspond to those in PSS, respectively. Although the shift of the S 2p peaks was less noticeable between untreated and DMSO-treated nanofilms, in the case of DMSO/HZ-treated

nanofilms, the shift of the lower energy peaks for PSS was observed, indicating that the sulfonic acid groups ( $-\text{SO}_3\text{H}^+$ ) interacted with HZ to form the complex ( $-\text{SO}_3^-\text{N}_2\text{H}_5^+$ ). The similar low energy shift of the S atoms in PEDOT was also observed, suggesting that the electrostatic interaction between PEDOT and PSS units might be weaker due to the presence of DMSO and/or HZ between PEDOT and PSS.<sup>37, 39, 40</sup> The main peak in the carbon (C) 1s spectra is fitted with four peaks at 284.72, 285.8, 286.75 and 287.95 eV, which are associated with C–C/C–H, C–S, C=C–O and C–O–C/C–O, respectively. This result is in good agreement with the previous report.<sup>41, 42</sup>

For the oxygen (O) 1s spectra as shown in **Figure 5**, the bimodal peak can be depicted in two peaks at around 530-535 eV corresponding to the oxygen atoms in the PEDOT units in higher binding energy regions (533 eV), whereas the oxygen atoms in the PSS units give their characteristic peaks in relatively lower binding energy regions (531 eV). While no shift of low energy peaks was observed in the case of PEDOT, a huge change of the shape and a shift of the peaks were appeared for the PSS region. The change of the peaks for the O 1s of the PSS units confirms that HZ interacts with the sulfonic acid groups of PSS chain for neutralization after treatment of mixtures of DMSO/HZ. Finally, large nitrogen (N) 1s peak from HZ was detected in the mixture-treated nanofilms, whereas almost no N 1s peak was found in untreated and DMSO-added nanofilms.

The ultraviolet-visible-near-infrared (UV-Vis-NIR) absorption spectra of the PEDOT:PSS

nanofilms indicate a systematic change of the optical spectra depending on the chemical doping level (**Figure 6**). This systematic control of the doping level was obtained by treating the PEDOT:PSS nanofilms with an over-coating process of a composition-controlled DMSO/HZ solution for 10 seconds. Upon dedoping with a mixture of DMSO/HZ, the dedoped PEDOT:PSS nanofilms changed the color from light blue to dark blue (**Figure 6b**). The dedoping process of PEDOT:PSS nanofilms gradually eliminated the (bi)polaronic optical transitions in the IR region, while new optical transitions in the visible region appeared (around 600 nm). The pristine and DMSO-added PEDOT:PSS nanofilms exhibit a broad infrared absorption band around 900 nm, a feature typically seen in the polaron state of conducting polymers.<sup>43</sup> It is a result of the polaronic band formation.<sup>44</sup> The NIR transitions above 900 nm were attributed to interacting bipolarons. No significant change was observed in the visible region of the absorption spectra of the DMSO-added PEDOT:PSS nanofilms. As the HZ composition increased, the broad IR absorption background drastically diminished in intensity while a broad polaronic transitions peak increased at 850–900 nm. The DMSO/HZ solution induced a polaron absorption band during the over-coating, showing the dedoping of PEDOT chains. Simultaneously, new transitions evolved at around 600 nm that originated from the absorption of neutral PEDOT segments.

**Figure 7** shows the thermoelectric properties of the PEDOT:PSS nanofilms, dedoped with a mixture of DMSO/HZ and of water/HZ, as a function of HZ compositions of the over-coating

solution. The nanofilms treated with DMSO without HZ (0 wt% of HZ in DMSO) shows an electrical conductivity of 726 S/cm, which is 10 times higher than that of the pristine nanofilms (70 S/cm) and a Seebeck coefficient of 30  $\mu\text{V/K}$ , which is slightly lower in the pristine (34  $\mu\text{V/K}$ ). Aprotic polar solvents with a high dielectric constant, such as DMSO, induce the stronger screening effect between charge carriers and counter ions, resulting in reduction of the Coulomb interaction between positively charged PEDOT and negatively charged PSS primary dopants. The PEDOT:PSS nanofilms can be further chemically dedoped by over-coating the mixture of DMSO and a small amount of HZ onto the nanofilms. The mixture of DMSO/HZ penetrated into intermolecular sites between PEDOT and PSS, resulting in the large dedoping effect. The Hall mobility and charge-carrier concentration, both obtained by the Hall-effect measurement, supported the effect of dedoping processes (Figure S2). The Hall mobility increased after addition of DMSO, whereas the carrier concentration was not changed. However, when the nanofilm was dedoped by over-coating with a DMSO/HZ mixture, the carrier concentration decreased and the mobility increased as the amount of HZ in the over-coating solution increased.

The electrical conductivity of dedoped nanofilms gradually decreased from 726 S/cm to 2 S/cm with increasing HZ composition from 0 to 3.2 wt%, while the Seebeck coefficient increased at the same time from 30 to 142  $\mu\text{V/K}$ . The nanofilms dedoped by a water/HZ mixture showed similar trends of the electrical conductivity and the Seebeck coefficient as a



function of HZ composition, although the degree of changes was smaller compared to the case of DMSO/HZ-based dedoping system (**Figure 7b**). We note that, because the thickness of the dedoped PEDOT:PSS nanofilms is almost identical ( $\sim 274 \pm 14$  nm) regardless of the DMSO/HZ concentration, we have not considered any thickness effect on the thermoelectric properties of the nanofilms in this study. Although it is usual to observe an inverse relationship between the Seebeck coefficient and the electrical conductivity,<sup>19, 20</sup> we obtained a larger increase in the Seebeck coefficient than a decrease in the electrical conductivity, resulting in the power factor that peaked after chemical dedoping of PEDOT:PSS nanofilms with 0.0175 wt% HZ in the mixture. The highest power factor of  $112 \mu\text{W}/\text{mK}^2$  is  $\sim 14$  times larger than that of the pristine PEDOT:PSS nanofilms in this study ( $8 \mu\text{W}/\text{mK}^2$ ), and  $\sim 2$  times of the DMSO-treated PEDOT:PSS nanofilms ( $65 \mu\text{W}/\text{mK}^2$ ). We calculated the thermoelectric figure-of-merits of the nanofilms with the power factors obtained above and the thermal conductivity measured by using the Laser Flash Apparatus (LFA) methods (Table 1). The thermoelectric figure-of-merit,  $ZT$ , of dedoped nanofilms was as high as 0.093 at room temperature, which is  $\sim 13.2$  times higher than that of the pristine PEDOT:PSS nanofilms ( $ZT=0.007$ ) and  $\sim 1.5$  times of the DMSO-treated PEDOT:PSS nanofilms ( $ZT=0.063$ ). The drastic enhancement of  $ZT$  in the dedoped nanofilms proves the power of our over-coating/dedoping process.

## 4. Conclusions

In summary, we have demonstrated that *chemical* dedoping and molecular reorganization of PEDOT:PSS in the nanofilms by an over-coating step results in the enhanced thermoelectric properties. The Seebeck coefficient of the highly conductive PEDOT:PSS nanofilms was increased by using a mixture of DMSO/HZ as two mediators. Despite a decrease in the electrical conductivity upon chemical dedoping, the power factor in the PEDOT:PSS system was increased to  $112 \mu\text{W}/\text{mK}^2$  due to a larger increase in the Seebeck coefficient. Systematic studies of Raman, XPS, and UV-Vis-NIR spectra as well as surface morphology and thermoelectric properties revealed that conformational changes and chemical dedoping are responsible for the enhancement of the power factors. We believe that this simple chemical processing is generally applicable to other thermoelectric systems based on conducting polymers to increase the thermoelectric energy conversion efficiency.

## Acknowledgements

This research was supported by Nano-Material Technology Development Program through the National Research Foundation of Korea (NRF) funded by the Ministry of Education, Science and Technology (2008-2002380/2012-0006227) and the Pioneer Research Center Program through the NRF funded by the Ministry of Science, ICT & Future Planning (2010-0019550). This work was also supported by Priority Research Centers Program through the

NRF funded by the Ministry of Education, Science and Technology (2009-0093823), the Converging Center Program through the Ministry of Education, Science and Technology (2010K001430), and the Yonsei University Research Fund of 2013 (in part).

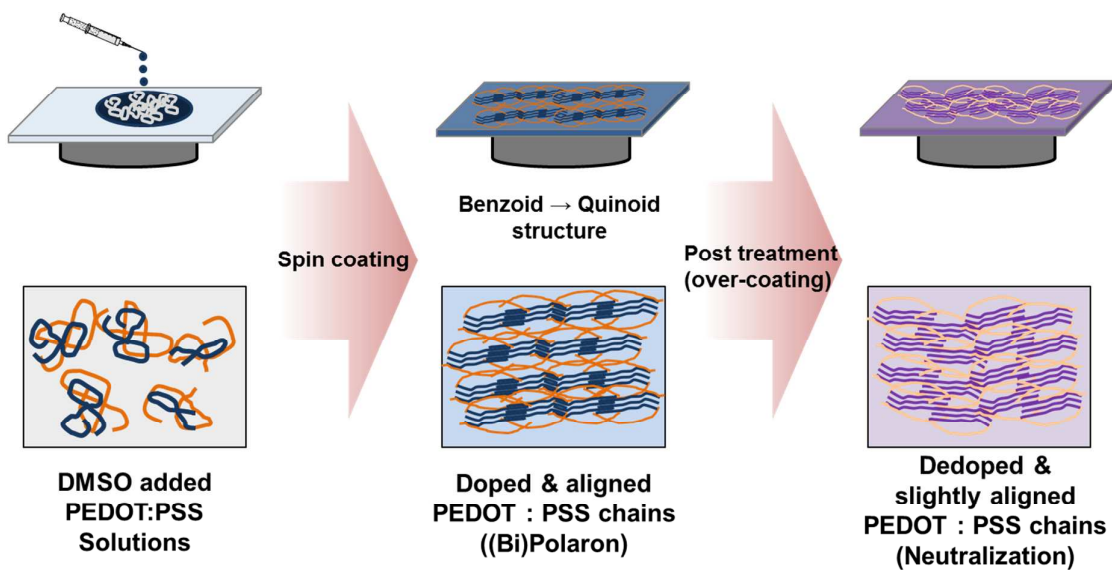
## REFERENCES

1. D. M. Rowe, *CRC handbook of thermoelectrics*, CRC press, Boca Raton, 2006.
2. J. P. Fleurial, A. Borshchevsky, T. Caillat and R. Ewell, *Proc. Intersoc. Energy Convers. Eng. Conf*, 1997, **2**, 1080.
3. G. J. Snyder and E. S. Toberer, *Nat. Mater*, 2008, **7**, 105.
4. M. Vosgueritchian, D. J. Lipomi and Z. Bao, *Adv. Funct. Mater.*, 2012, **22**, 421.
5. R. Yue and J. Xu, *Synth. Met.*, 2012, **162**, 912.
6. J. Feng-Xing, X. Jing-Kun, L. Bao-Yang, X. Yu, H. Rong-Jin, L. Lai-Feng, *Chin. Phys. Lett.*, 2008, **25**, 2202.
7. N. Dubey and M. Leclerc, *J. Polym. Sci., Part B: Polym. Phys.*, 2011, **49**, 467.
8. B. Zhang, J. Sun, H. Katz, F. Fang and R. Opila, *ACS Appl. Mater. Interfaces*, 2010, **2**, 3170.
9. D. Maddison, J. Unsworth and R. Roberts, *Synth. Met.*, 1988, **26**, 99.
10. F. Yakuphanoglu and B. Senkal, *J. Phys. Chem. C*, 2007, **111**, 1840.
11. H. Yan, T. Ohta and N. Toshima, *Macromol. Mater. Eng.*, 2001, **286**, 139.

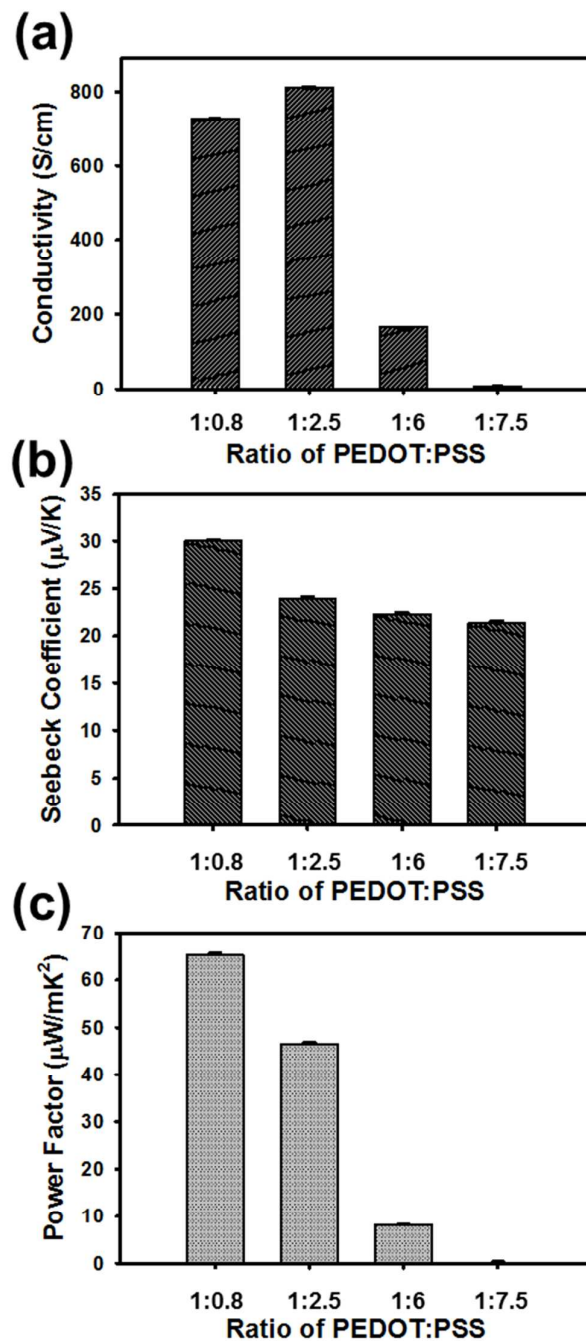
12. R. d. B. Aïch, N. Blouin, A. I. Bouchard and M. Leclerc, *Chem. Mater.*, 2009, **21**, 751.
13. L. Bao-Yang, L. Cong-Cong, L. Shan, X. Jing-Kun, J. Feng-Xing, L. Yu-Zhen and Z. Zhuo, *Chin. Phys. Lett.*, 2010, **27**, 057201.
14. J. Sun, M.-L. Yeh, B. Jung, B. Zhang, J. Feser, A. Majumdar and H. Katz, *Macromolecules*, 2010, **43**, 2897.
15. Y. Shinohara, K. Ohara, H. Nakanishi, Y. Imai and Y. Isoda, *Mater. Sci. Forum*, 2005, **492-493**, 141.
16. O. Bubnova, Z. U. Khan, A. Malti, S. Braun, M. Fahlman, M. Berggren and X. Crispin, *Nat. Mater.*, 2011, **10**, 429.
17. C. Liu, F. Jiang, M. Huang, R. Yue, B. Lu, J. Xu and G. Liu, *J. Electron. Mater.*, 2011, **40**, 648.
18. C. Liu, J. Xu, B. Lu, R. Yue and F. Kong, *J. Electron. Mater.*, 2012, **41**, 639.
19. T.-C. Tsai, H.-C. Chang, C.-H. Chen and W.-T. Whang, *Org. Electron.*, 2011, **12**, 2159.
20. O. Bubnova, M. Berggren and X. Crispin, *J. Am. Chem. Soc.*, 2012, **134**, 16456.
21. S. I. Na, S. S. Kim, J. Jo and D. Y. Kim, *Adv. Mater.*, 2008, **20**, 4061.
22. X. Crispin, F. Jakobsson, A. Crispin, P. Grim, P. Andersson, A. Volodin, C. Van Haesendonck, M. Van der Auweraer, W. R. Salaneck and M. Berggren, *Chem. Mater.*, 2006, **18**, 4354.
23. S. Jönsson, J. Birgerson, X. Crispin, G. Greczynski, W. Osikowicz, A. Denier Van Der

- Gon, W. R. Salaneck and M. Fahlman, *Synth. Met.*, 2003, **139**, 1.
24. Y. H. Kim, C. Sachse, M. L. Machala, C. May, L. Müller-Meskamp and K. Leo, *Adv. Funct. Mater.*, 2011, **21**, 1076.
25. Y. Wang, K. Cai and X. Yao, *ACS Appl. Mater. Interfaces*, 2011, **3**, 1163.
26. C. Liu, B. Lu, J. Yan, J. Xu, R. Yue, Z. Zhu, S. Zhou, X. Hu, Z. Zhang and P. Chen, *Synth. Met.*, 2010, **160**, 2481.
27. F. Kong, C. Liu, J. Xu, Y. Huang, J. Wang and Z. Sun, *J. Electron. Mater.*, 2012, **41**, 2431.
28. J. Luo, D. Billep, T. Waechtler, T. Otto, M. Toader, O. Gordan, E. Sheremet, J. Martin, M. Hietschold, D. R. T. Zahn and T. Gessner, *J. Mater. Chem. A*, 2013, **1**, 7576.
29. S. K. Yee, N. E. Coates, A. Majumdar, J. J. Urban and R. A. Segalman, *Phys. Chem. Chem. Phys.*, 2013, **15**, 4024.
30. G. H. Kim, L. Shao, K. Zhang and K. P. Pipe, *Nat. Mater.*, 2013, **12**, 719.
31. W. Lövenich, R. Hill, *WO2011015364*, 2010 (Germany).
32. S. Garreau, G. Louarn, J. Buisson, G. Froyer and S. Lefrant, *Macromolecules*, 1999, **32**, 6807.
33. M. Łapkowski and A. Proń, *Synth. Met.*, 2000, **110**, 79.
34. S. Garreau, J. Duvail and G. Louarn, *Synth. Met.*, 2001, **125**, 325.
35. J. Ouyang, Q. Xu, C.-W. Chu, Y. Yang, G. Li and J. Shinar, *Polymer*, 2004, **45**, 8443.

36. J. Ouyang, C.-W. Chu, F. C. Chen, Q. Xu and Y. Yang, *Adv. Funct. Mater.*, 2005, **15**, 203.
37. G. Greczynski, T. Kugler and W. Salaneck, *Thin Solid Films*, 1999, **354**, 129.
38. G. Zotti, S. Zecchin, G. Schiavon, F. Louwet, L. Groenendaal, X. Crispin, W. Osikowicz, W. Salaneck and M. Fahlman, *Macromolecules*, 2003, **36**, 3337.
39. J. Hwang, F. Amy and A. Kahn, *Org. Electron.*, 2006, **7**, 387.
40. H. Yan and H. Okuzaki, *Synth. Met.*, 2009, **159**, 2225.
41. M. Khan, S. Armes, C. Perruchot, H. Ouamara, M. Chehimi, S. Greaves and J. Watts, *Langmuir*, 2000, **16**, 4171.
42. S. A. Spanninga, D. C. Martin and Z. Chen, *J. Phys. Chem. C*, 2009, **113**, 5585.
43. H. J. Ahonen, J. Lukkari and J. Kankare, *Macromolecules*, 2000, **33**, 6787.
44. M. M. de Kok, M. Buechel, S. I. E. Vulto, P. van de Weijer, E. A. Meulenkaamp, S. H. P. M. de Winter, A. J. G. Mank, H. J. M. Vorstenbosch, C. H. L. Weijtens and V. van Elsbergen, *phys. stat. sol. (a)*, 2004, **201**, 1342.

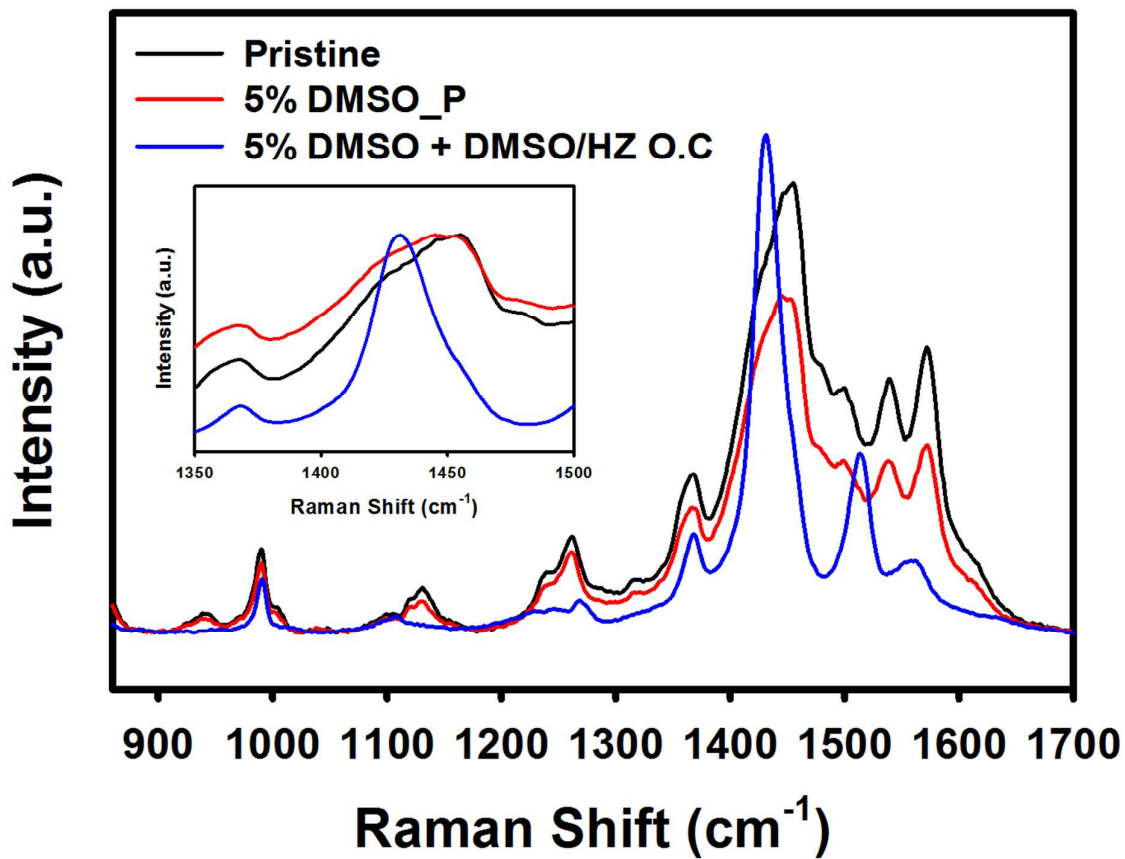


**Figure 1.** Schematic diagram of the dedoping procedure of PEDOT:PSS nanofilms by using over-coating and dedoping methods.

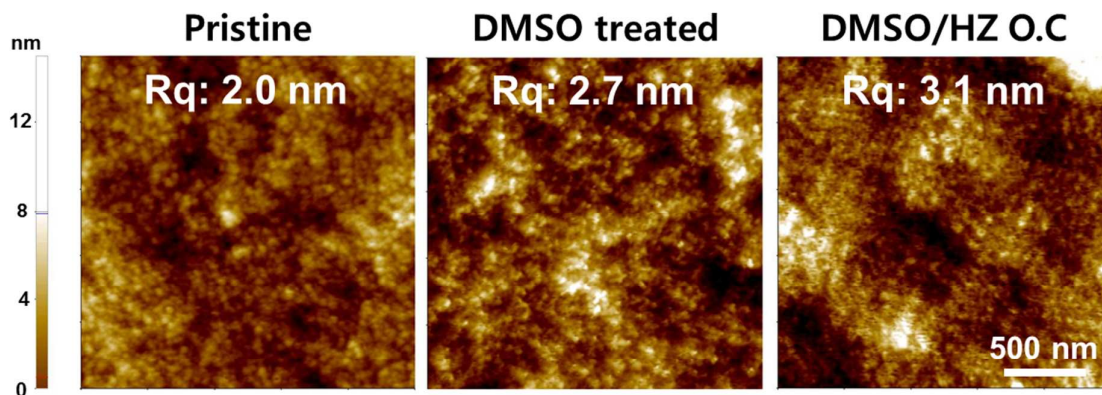


**Figure 2.** Thermoelectric properties of PEDOT:PSS nanofilms with various PEDOT to PSS ratios: (a) electric conductivity, (b) Seebeck coefficient, and (c) power factor of PEDOT:PSS nanofilms.

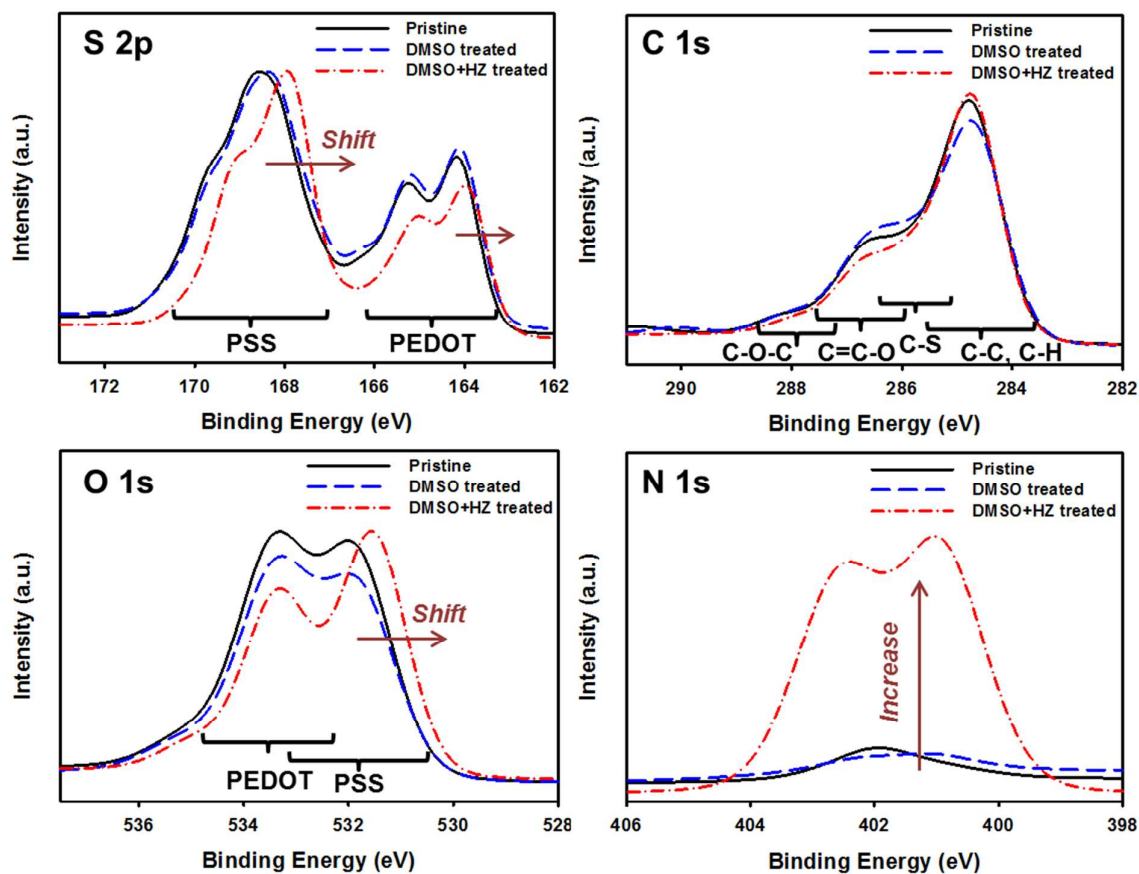




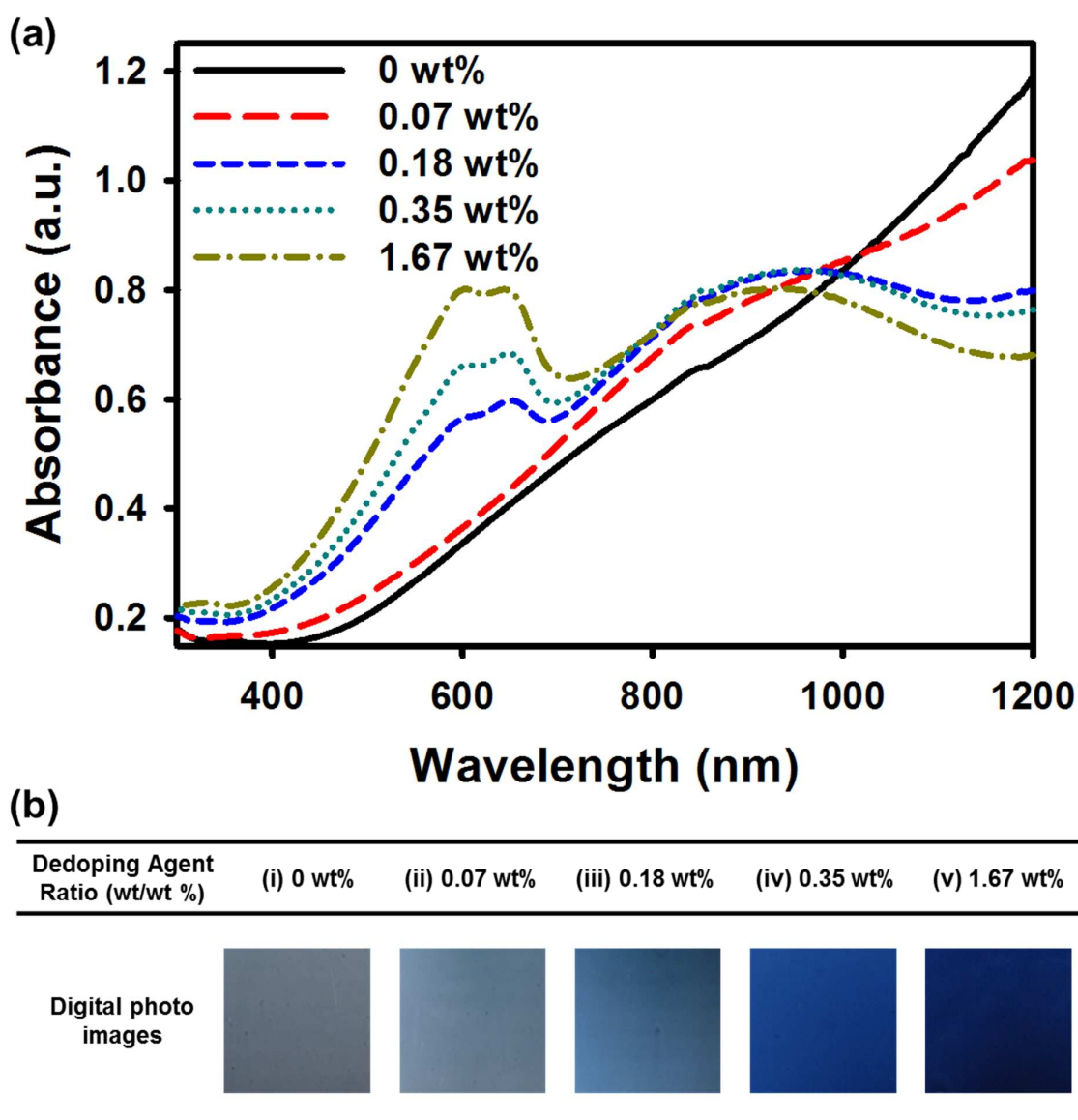
**Figure 3.** Raman spectra of PEDOT:PSS nanofilms under 532 nm laser excitation as a function of the DMSO treatment and the DMSO/HZ treatment.



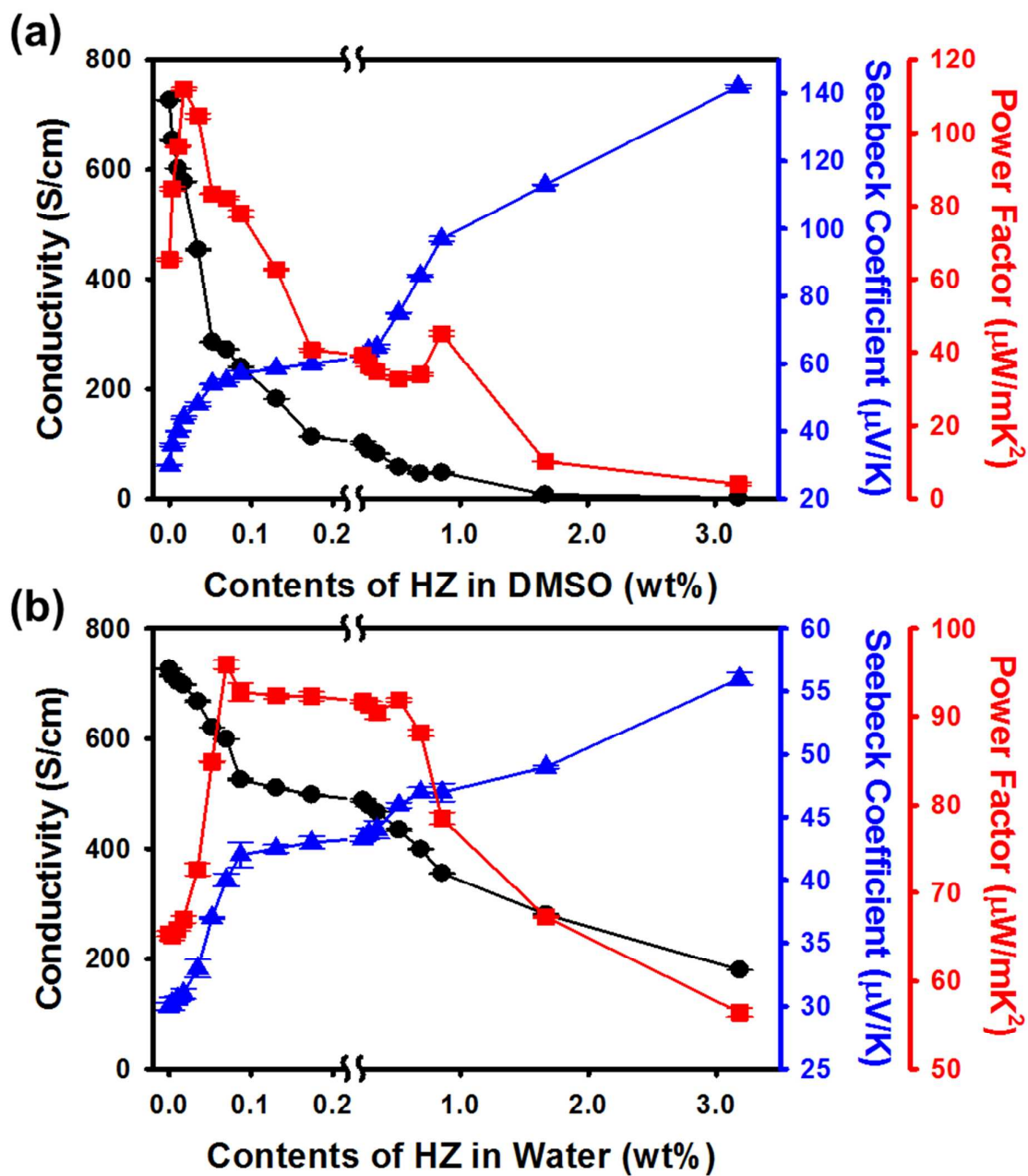
**Figure 4.** AFM topographic images of PEDOT:PSS nanofilms: (a) pristine, (b) DMSO-treated, and (c) treated with a mixture of DMSO/HZ. All images captured an area of  $2 \times 2 \mu\text{m}^2$ .



**Figure 5.** X-ray photoelectron spectra (XPS) of pristine, DMSO-treated and DMSO/HZ-mixture treated PEDOT:PSS nanofilms.



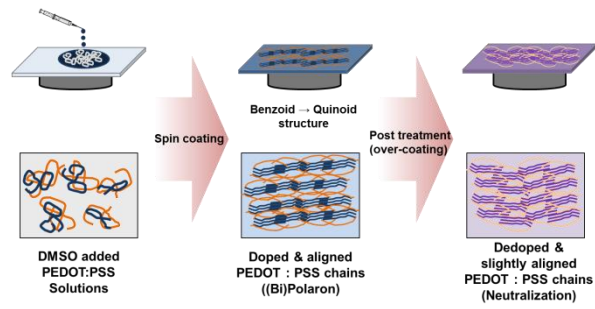
**Figure 6.** UV-Vis-NIR spectra (a) and digital photographic images (b) of DMSO and DMSO/HZ-mixture-treated PEDOT:PSS nanofilms with different ratios of mixture solutions.



**Figure 7.** Thermoelectric parameters of dedoped PEDOT:PSS nanofilms as a function of compositions of the dedoping agents in DMSO (a) or in water (b) used for over-coating.

**Table 1.** Thermal properties of PEDOT:PSS nanofilms measured by a laser flash method at room temperature.

	Thermal Diffusivity ( $D$ ; mm <sup>2</sup> /s)	Specific Heat ( $C_p$ ; J/(g K))	Density ( $d$ ; g/cm <sup>3</sup> )	Thermal Conductivity ( $\kappa$ ; W/(m K))
Pristine	0.216	1.175	1.373	0.348 ± 0.01
DMSO treated PEDOT:PSS	0.166	1.415	1.327	0.312 ± 0.019
DMSO/HZ treated PEDOT:PSS	0.187	1.415	1.385	0.366 ± 0.016

**A table of contents entry (TOC)**

Our results indicate that a well-designed simple post-processing can boost the efficiency of thermoelectric power generators made of conjugated polymer thin films.

Our results indicate that a well-designed simple post-processing can boost the efficiency of thermoelectric power generators made of conjugated polymer thin films.